Available online at www.sciencedirect.com
SCIENCE DIRECT®
Optics Communications 227 (2003) 193–202
OPTICS COMMUNICATIONS
www.elsevier.com/locate/optcom

Two-dimensional soliton-induced refractive index change in photorefractive crystals

G.F. Calvo [a], F. Agulló-López [a], M. Carrascosa [a], M.R. Belić [b,*], D. Vujić [b,1]

[a] Departamento de Física de Materiales C-IV, Universidad Autónoma de Madrid Cantoblanco, Madrid E-28049, Spain
[b] Institute of Physics, P.O. Box 57, Belgrade 11001, Yugoslavia

Received 26 February 2003; received in revised form 6 June 2003; accepted 8 September 2003

Abstract

An analysis of light-induced space-charge field, valid for the propagation of two-dimensional solitons in photorefractive (PR) crystals, is carried out. Under conditions appropriate to the formation of self-trapped beams, the equation for the electrostatic potential is simplified and solved, to obtain an analytical expression for the space-charge field, and thus the refractive index change. The expression exhibits an excellent agreement with the numerical calculation for a variety of localized two-dimensional light beams, in particular for the bright fundamental and higher-order vortex spatial screening solitary waves. Based on analytical results, a class of models for the local isotropic two-dimensional space-charge field is proposed. They are compared to the general nonlocal anisotropic model, using the propagation and breakup of vortex beams as an example.

PACS: 42.65.Tg; 42.65.Hw

1. Introduction

Self-trapped optical beams in photorefractive (PR) materials have been the subject of intense research effort in the past decade [1]. They arise when diffraction is compensated by nonlinearity in PR media, leading to the formation of optical solitons. The PR effect results from the excitation, transport, and trapping of free carriers, which give rise to the build-up of space-charge field, that in turn modulates the refractive index by means of the linear electro-optic (i.e., Pockels) effect. The PR effect allows for the self-trapping in one and two transverse dimensions at very low optical power levels (microwatts). Both one-dimensional (1D) and two-dimensional (2D) spatial solitary waves have a unique shape which is determined

* Corresponding author. Fax: +381-11-3162-190.
E-mail address: belic@phy.bg.ac.yu (M.R. Belić).
[1] Present address: Department of Physics, University of Toronto, Toronto, ON, M5S 1A7, Canada.

0030-4018/$ - see front matter
doi:10.1016/j.optcom.2003.09.061

by the strength of the external electric field, the light intensity, and the beam diameter. However, the situation with the 2D case is considerably more complicated [2–4].

The complication is that, although self-focusing of the beam takes place in two transverse directions, the external field necessary for the screening effect is applied along only one transverse direction. As a rule, this is the direction in which the electro-optic effect is maximal, according to the anisotropic character of the dielectric tensor. This anisotropy does not allow for circularly symmetric solitary waves. The overall structure of the refractive index makes the beams squeezed in the direction of the applied field. The higher dimensionality introduces a new feature, a nonlocal contribution to the light-induced refractive index, in contrast to the one dimensional situation, where the refractive index is local (i.e., it follows the local spatial dependence of the light intensity).

Our aim is to obtain a general analytical expression for the light-induced space-charge field and the change in the refractive index of the crystal that agrees well with the numerical calculation. Based on that expression we propose a novel form for the local isotropic part of the space-charge field that is better suited for the propagation of 2D self-trapped beams. We compare different isotropic models with each other and with the general anisotropic model, using the break-up of vortex solitons as an example.

Section 2 of the paper introduces a model for material equations, Section 3 contains an analysis of the equations, Section 4 presents results, Section 5 offers a discussion, Section 6 considers the propagation of beams, and Section 7 gives conclusions.

2. Model

The starting point is the standard one-trap model for electrons as the sole charge transport mechanism [5]. For our purposes, the material equations (Kukhtarev's equations) that describe the PR effect will be written in a slightly different form [2], by introducing an electrostatic potential ϕ that corresponds to the space-charge field $\mathbf{E}_{\mathrm{sc}} = -\nabla\phi$:

$$\partial_t N_{\mathrm{D}}^{+} = S(1+I)(N_{\mathrm{D}} - N_{\mathrm{D}}^{+}) - \gamma_{\mathrm{r}} n_{\mathrm{e}} N_{\mathrm{D}}^{+}, \tag{1a}$$

$$-\epsilon_0\epsilon_{\mathrm{r}}\nabla^2\phi = \rho, \tag{1b}$$

$$\partial_t\rho + \nabla\cdot\mathbf{j} = 0. \tag{1c}$$

Here N_{D}^{+} stands for the density of ionized donors, I is the light intensity of the propagating beam (in units of the saturation intensity), n_{e} is the free-electron density, S and γ_{r} are the photoexcitation and recombination constants, N_{D} and N_{A} are the concentrations of donors and acceptors, $\rho = q(N_{\mathrm{D}}^{+} - N_{\mathrm{A}} - n_{\mathrm{e}})$ is the charge density, $\mathbf{j} = -\mu q n_{\mathrm{e}}\nabla\phi + \mu k_{\mathrm{B}} T\nabla n_{\mathrm{e}}$ is the current density, μ is the electron mobility, q is the carrier charge, T is the absolute temperature, k_{B} is Boltzmann's constant, ϵ_{r} and ϵ_0 are the scalar dielectric constants of the material and vacuum, respectively. Thus, the model essentially consists of the equation for the generation/recombination of mobile charges, the Poisson equation for the charge density, and the continuity equation for the current density. We proceed to analyze them.

3. Analysis

The quantity of essential interest is the potential ϕ. A closed-form time-dependent equation for ϕ is obtained by substituting Eq. (1b) into Eq. (1c)

$$\partial_t(\nabla^2\phi) = \frac{\mu}{\epsilon_0\epsilon_{\mathrm{r}}}\left(q n_{\mathrm{e}}\nabla^2\phi + q\nabla n_{\mathrm{e}}\cdot\nabla\phi + k_{\mathrm{B}} T\nabla^2 n_{\mathrm{e}}\right). \tag{2}$$

To induce the formation of screened sparial solitons it is necessary to apply an external electric field E_0 across the crystal. In a standard geometry the field is applied along the x-axis, orthogonally to the beam propagation direction, which is taken to be the z-axis. This makes the potential satisfy the following boundary condition:

$$\phi\left(\frac{l}{2}\right) - \phi\left(-\frac{l}{2}\right) = E_0 l, \tag{3}$$

where l is the distance measured along the x-axis between the two crystal faces to which the external bias voltage is applied. Further analysis requires an expression for n_e in terms of the known quantities.

It is assumed that the recombination/generation process reaches equilibrium much faster than other processes in the crystal, which means $\partial_t N_D^+ = 0$. Inserting the expression for $N_D^+ = \rho/q + N_A + n_e$ into the steady-state Eq. (1a), one obtains a quadratic equation for n_e:

$$n_e = n_I \frac{N_D - N_A - \rho/q - n_e}{N_A + \rho/q + n_e}, \tag{4}$$

where $n_I = S(1+I)/\gamma_r$ is the fraction of electron density proportional to the light intensity. This equation is solved either directly or iteratively, by inserting the zeroth-order approximation $n_e^{(0)} = n_I(N_D - N_A)/N_A$ into the right-hand side, and continuing the process. However, by arguing that $(\rho/q + n_e)/N_A$ is already small [6], the zeroth-order approximation is found quite satisfactory. Hence one can write

$$n_e \approx \frac{S(N_D - N_A)}{\gamma_r N_A}(1+I), \tag{5}$$

which is much explored in the modeling.

Inserting Eq. (5) into (2), and after some rearranging, an intensity-dependent potential equation is obtained

$$\tau\partial_t(\nabla^2\varphi) = \nabla^2\varphi + \nabla\ln(1+I)\cdot\nabla\varphi - E_0\partial_x\ln(1+I) - \frac{k_B T}{q}\left\{\nabla^2\ln(1+I) + [\nabla\ln(1+I)]^2\right\}, \tag{6}$$

where

$$\tau = \frac{\epsilon_0\epsilon_r\gamma_r N_A}{\mu q S(1+I)(N_D - N_A)}, \tag{7}$$

is the intensity-dependent relaxation time of the crystal, and we have redefined the potential $\phi \equiv \varphi + E_0 x$, so that the boundary conditions are now $\varphi \to 0$ for x,y large. The last two terms in Eq. (6) represent the drift of charge carriers under the space-charge field and the diffusion field of the crystal. The charge-carrier diffusion term is responsible for the bending of light beams as they propagate through the crystal.

In what follows we shall restrict ourselves to the steady-state situation $\partial_t(\nabla^2\varphi) = 0$, and thus consider the electrostatic potential equation

$$\nabla^2\varphi + \nabla\ln(1+I)\cdot\nabla\varphi = E_0\partial_x\ln(1+I) + \frac{k_B T}{q}\left\{\nabla^2\ln(1+I) + [\nabla\ln(1+I)]^2\right\}. \tag{8}$$

It should be noted that the most troublesome for the treatment of Eq. (8) is the second term on the left hand side. Without it the equation reduces to Poisson's equation. In [3] the solution to Eq. (8) is obtained by neglecting the second term. We follow a different route.

4. Results

It is interesting to note that Eq. (8) can be solved exactly in the transverse 1D case (x coordinate only), giving rise to a space-charge field of the form

$$E_{sc}(x) = E_0 \frac{1+I_\infty}{1+I} - \frac{k_B T}{q} \frac{\mathrm{d}\ln(1+I)}{\mathrm{d}x}, \tag{9}$$

where I_∞ is the value of intensity at the infinity. Since the light-induced refractive index change is given in terms of the space-charge field as $\Delta n = n_0^3 r_{\mathrm{eff}} E_{sc}/2$, where n_0 is the unperturbed refractive index of the material and r_{eff} is the effective electro-optic coefficient along the applied field direction, we can see from Eq. (9) that, apart from the diffusion contribution, the refractive index change displays the well known $(1+I)^{-1}$ dependence and, also, a local behavior, i.e., it depends on the local values of intensity.

In the 2D case, Eq. (8) cannot be solved in closed form. Nevertheless, under some appropriate assumptions, it is still possible to obtain a general analytical expression for the space-charge field that exhibits a remarkable agreement with the numerical calculations. First, we simplify Eq. (8) by making the following transformation of the potential

$$\varphi(x,y) = E_0 \frac{u(x,y)}{\sqrt{1+I}} + \frac{k_B T}{q} \ln(1+I), \tag{10}$$

where the new modified potential $u(x,y)$ satisfies the canonical elliptic equation

$$\nabla^2 u - \left[\nabla^2 \ln\sqrt{1+I} + \left(\nabla \ln\sqrt{1+I}\right)^2\right] u = 2\partial_x \sqrt{1+I}. \tag{11}$$

The usefulness of the above transformation is based on the fact that for the well localized beams in 2D, that is when the intensity I decays fast in both x and y directions, it is a better approximation to neglect the second term on the left hand side of Eq. (11) than to neglect the second term on the left hand side of Eq. (8). In this manner one obtains an excellent approximation to the full numerical solution, as it will be seen below, that can be treated analytically. Hence, we restrict ourselves to solving the Poisson equation

$$\nabla^2 u = 2\partial_x \sqrt{1+I}, \tag{12}$$

in terms of the 2D Green's function

$$u(x,y) = \frac{1}{\pi} \int_{-\infty}^{\infty} \int_{-\infty}^{\infty} \left[\frac{\partial}{\partial \xi} \sqrt{1+I(\xi,\eta)}\right] \ln\sqrt{(x-\xi)^2 + (y-\eta)^2}\,\mathrm{d}\xi\ \mathrm{d}\eta. \tag{13}$$

Let us introduce polar coordinates, according to the expressions:

$$\rho\cos\theta = \xi - x, \tag{14a}$$

$$\rho\sin\theta = \eta - y \tag{14b}$$

(ρ here not to be confused with the charge density). Then, Eq. (13) can be integrated by parts, to yield

$$u(x,y) = -\frac{1}{\pi} \int_0^{\infty} \int_0^{2\pi} \sqrt{1+I(x+\rho\cos\theta, y+\rho\sin\theta)}\ \cos\theta\ \mathrm{d}\rho\ \mathrm{d}\theta. \tag{15}$$

We are now in position to check the correctness of the approximation, by comparing the analytical result, Eq. (15) with the numerical solution of Eq. (11). This is accomplished in Fig. 1, using light intensity distribution of a 2D vortex beam. It is seen that the agreement between the approximate solution and the numerical is strikingly good, especially if one takes into account that the cuts in Fig. 1 are actually made at the places where the agreement is the worst.

Notice that when x and/or $y \to \infty$, in the case of localized beams the intensity becomes independent of θ and $u \to 0$. Also, for centro-symmetric light intensity profiles, i.e., if $I(-x,-y) = I(x,y)$, it follows from Eq. (15) that $u(-x,-y) = -u(x,y)$ (as well as for $\phi(x,y)$). Our numerical simulations have shown that during the propagation process initial radially symmetric beams change into radially asymmetric beams. Nevertheless,

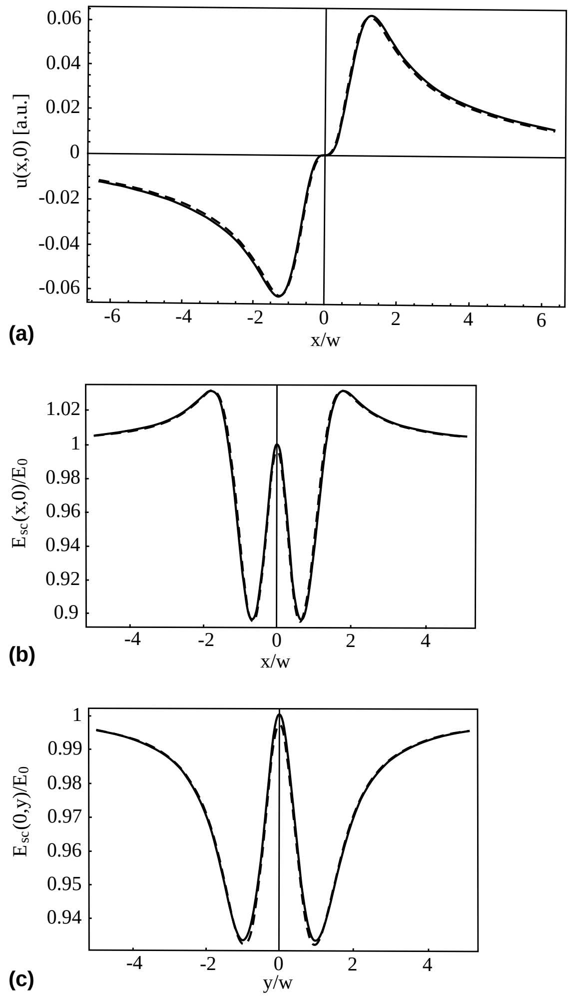

Fig. 1. Comparison of the numerical solution to Eq. (11) (dashed line) and the analytical formula Eq. (15) (full line), for a 2D vortex beam. (a) Modified potential along x direction. (b) Space-charge field along x, and (c) space-charge field along y axis.

inversion symmetry is still preserved. Using both properties implies that $\Delta n(-x,-y) = \Delta n(x,y)$ during the entire evolution of the beam (for $T = 0$).

Combining Eqs. (10) and (15), one obtains

$$\begin{aligned}\Delta n(x,y) = {} & \frac{1}{2} n_0^3 r_{\mathrm{eff}} \Bigg\{ -\frac{k_{\mathrm{B}} T}{\mathrm{e}} \partial_x \ln(1+I) \\ & \pm E_0 \Bigg\{ \frac{\sqrt{1+I_\infty}}{\sqrt{1+I}} \left[1 + \frac{1}{\pi} \int_0^\infty \int_0^{2\pi} \sqrt{1+I(x+\rho\cos\theta, y+\rho\sin\theta)} \frac{\cos 2\theta}{\rho} \, \mathrm{d}\rho \, \mathrm{d}\theta \right] \\ & - \frac{\partial_x \ln(1+I)}{2\pi\sqrt{1+I}} \int_0^\infty \int_0^{2\pi} \sqrt{1+I(x+\rho\cos\theta, y+\rho\sin\theta)} \, \cos\theta \, \mathrm{d}\rho \, \mathrm{d}\theta \Bigg\} \Bigg\},\end{aligned} \tag{16}$$

where the + sign corresponds to the self-focusing and the − sign to the self-defocusing nonlinearity. The expression in the curly brackets represents the space-charge field. This is the central result of the paper, and it warrants a discussion.

5. Discussion

Even though Eq. (16) is a closed-form expression, its analytical usefulness is obscured by complexity. Nonetheless, it can be used as a numerical tool, to estimate the refractive index distribution without solving the exact equations. Furthermore, it provides an interesting insight into the various contributions to the light-induced refractive index change. The most important term, the one proportional to $(1+I)^{-1/2}$, represents the contribution of the local isotropic part to $E_{\rm sc}$. It exhibits a different dependence on the light intensity, in comparison to what is found in the 1D case (see Eq. (9)). Of course, the inverse square-root dependence is restricted to the localized beams in 2D. As the beam increases its width along one direction relative to the other, there is a smooth transition to the $(1+I)^{-1}$ dependence. On the other hand, the two integrals in Eq. (16) constitute an evidence of the nonlocal contribution, i.e., the values of Δn at (x,y) are also influenced by the values of the intensity at points other than (x,y). This is a new feature not encountered in the 1D case. The nonlocal contribution gives rise to the appearance of adjacent lobes in the direction of external electric field, whose physical consequence is to introduce anisotropy and cause the light profile to loose radial symmetry. Apart from the above mentioned restrictions, Eq. (16) provides an excellent description for the refractive index induced by a large variety of light beams and, in particular, for the bright and dark solitary waves (they satisfy $I_\infty = 0$ and $I_\infty \neq 0$, respectively).

The form of Δn in Eq. (16) allows us to propose an improved model for the local isotropic space-charge field, to be used specifically for the 2D soliton propagation:

$$E_{\rm sc}(x,y) = E_0 \frac{\sqrt{1+I_\infty}}{\sqrt{1+I}} - \frac{k_{\rm B}T}{q}\partial_x \ln(1+I), \tag{17}$$

as opposed to the straightforward lifting of the 1D formula (Eq. (9)) to two transverse dimensions, which was utilized in numerous papers [7–11]. The advantage of the new model becomes apparent upon comparison with the full numerical solution of Eq. (8), presented in Fig. 2. As expected, the approximate expression (17) fails to describe the anisotropic features of the 2D photorefractive nonlinearity, visible in Fig. 2(a) in the form of protruding shoulders. The same applies to the inverse-intensity formula. However, the square-root formula represents very well the central local part of the refractive index change.

Owing to the action of the external field, anisotropic solitons are squeezed in the direction of the field, hence one can propose a class of saturable local models of the form

$$E_{\rm sc}(x,y) = E_0 \left(\frac{1+I_\infty}{1+I}\right)^{\alpha} - \frac{k_{\rm B}T}{q}\partial_x \ln(1+I), \tag{18}$$

that accounts for the cases between 1D and 2D, and deals adequately with the evolution of beams with different ellipticities. The parameter α is related to the ellipticity of a beam, $\alpha = 1/(1+w_x/w_y)$, with the values $1/2 \leqslant \alpha \leqslant 1$. The term w_x/w_y represents the ratio of beam diameters in the x and y directions. For $\alpha = 1/2$ the model is suitable for the circular beams, and for $\alpha = 1$ it is suitable for the striped beams.

6. Beam propagation

The space-charge field dependence on the light intensity represents only a half of the story of spatial solitons. The other half comes from the dependence of the light intensity, i.e., the beam envelope, on the

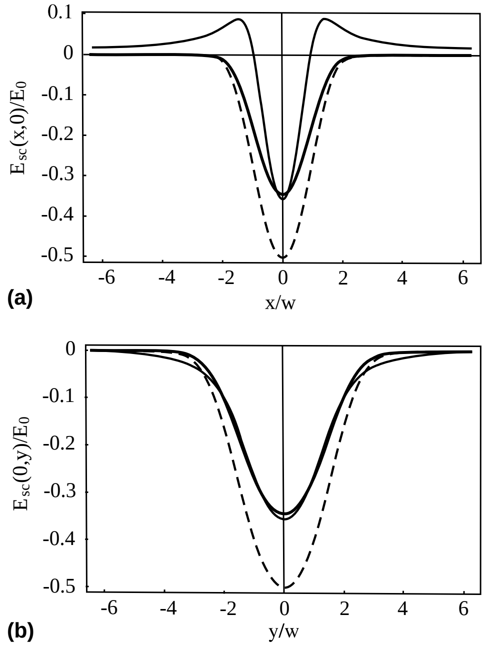

Fig. 2. Comparison of the numerical solution (full line) with the two local models, the square-root formula (heavy line) and the inverse-intensity formula (dashed line). The 2D space-charge field induced by a converged nonlocal soliton is fitted to a local elliptical Gaussian beam of ellipticity $\alpha = 0.76$ (a) along x-axis, (b) along y-axis.

space-charge field, and this is obtained by considering the paraxial wave equation for the beam propagation in the crystal. In this manner the problem is closed. The paraxial equation for the PR solitons is of the form

$$2ikn_0\partial_z A + \nabla^2 A = -k^2 n_0^4 r_{33} E_{sc} A, \tag{19}$$

where A is the beam envelope, k is the wave number in vacuum, n_0 is the bulk refractive index, and r_{33} the effective component of the electro-optic tensor that couples to the space-charge field. It is assumed that the beam propagates in the z-direction, and is polarized along the x-direction, which is also the direction of the crystalline c-axis.

We launch different initial beams into the crystal and compare the influence of local and nonlocal models for the space-charge field on the beam propagation. Two local models are utilized, the inverse-intensity formula, Eq. (9), and the square-root formula, Eq. (17). Launching simple Gaussian beams leads to subtle differences in the beam profile and similar propagation behavior in all the models. Hence we choose to launch vortex-mode solitons with different topological charges, whose behavior is much more model-dependent. The launching of more complex beams makes the isotropic models depart more from the anisotropic model. Still, the square-root formula provides for a better agreement with the anisotropic behavior than the inverse-intensity formula.

It is known [12] that a vortex beam cannot be the stable solitonic mode of propagation through the PR crystals, regardless of the model. Owing to the modulational instabilities, vortices self-focus into a number of filaments and disintegrate during propagation. According to the anisotropic model, as well as experiment [13], the vortex beam (of unit charge) decays within a fraction of diffraction length into two filaments, which rotate (clockwise or counterclockwise, depending on the sign of the charge) towards the stable equilibrium position, which is perpendicular to the direction of the external field. Afterwards the two beamlets oscillate about the stable direction and recede along the y-axis (Fig. 3). According to the local models, the behavior is considerably different.

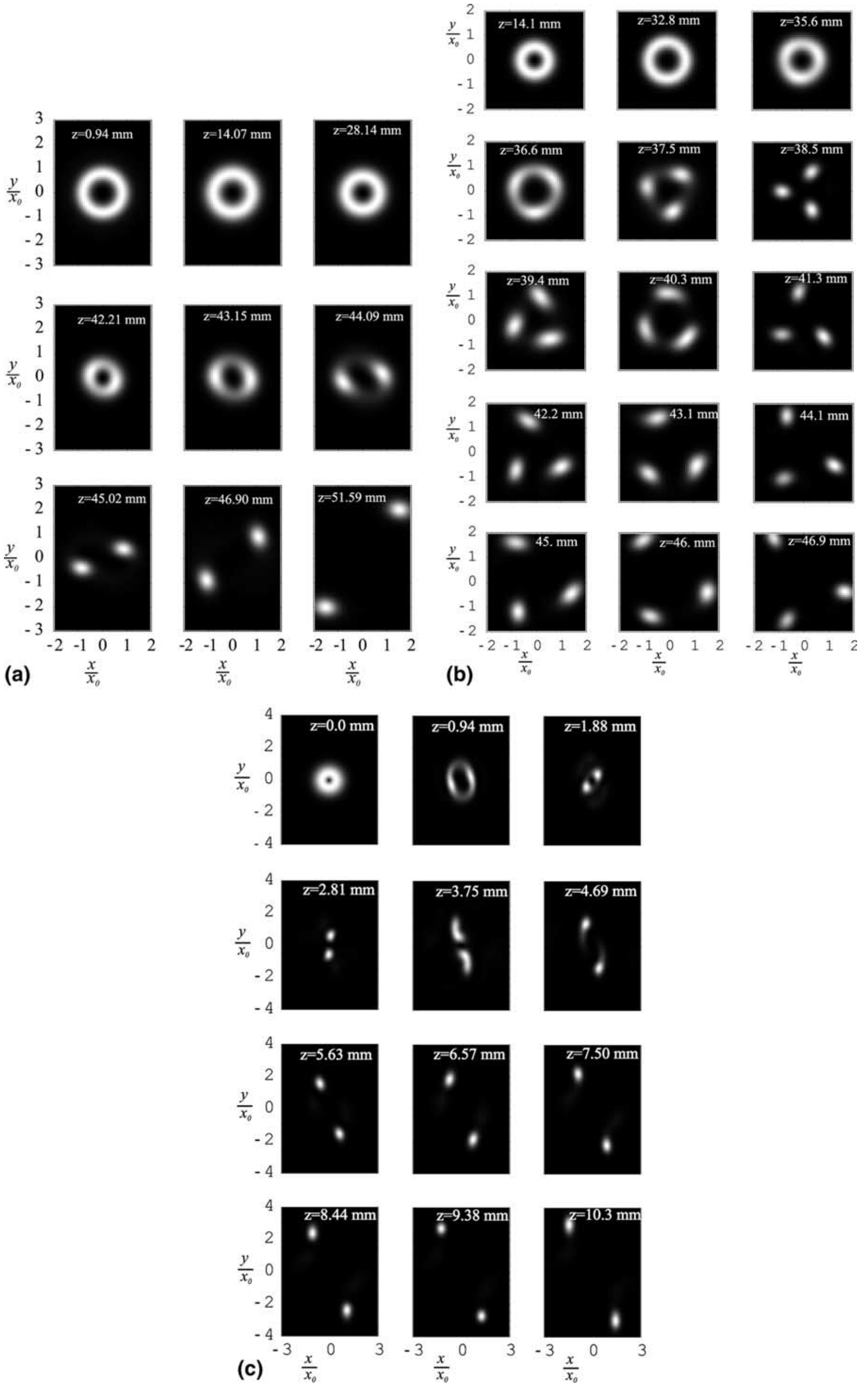

Fig. 3. Breakup of the vortex beam with unit topological charge. (a) Square-root model. (b) Inverse-intensity model. (c) Anisotropic model. The initial beam profile is the same in all three cases, and is visible in (c). Note widely different propagation distances for the isotropic and anisotropic models.

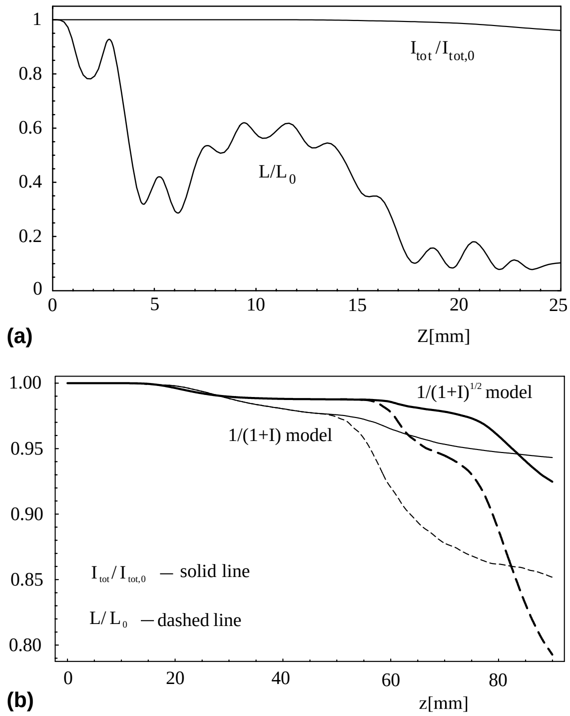

Fig. 4. Angular momentum and power of the vortices in (a) anisotropic and (b) isotropic models. Solid lines correspond to the power, dashed to the momentum of beams.

The propagation of vortices in isotropic models is much more stable. They can propagate for tens of diffraction lengths before disintegrating. Such a drastic difference in the behavior of anisotropic and isotropic models points to the inadequacy of describing vortex beams in PR crystals using local models. Nonetheless, when the isotropic vortices eventually reach the break-up phase, the breaking of the square-root model proceeds in stages similar to the anisotropic model, except that there exists no symmetry-breaking stable direction in which the fragments would fly apart. Hence the vortex fragments initially rotate about each other and then recede along straight paths that bear no clear relation to the external field. The break-up of the inverse-intensity model proceeds in a more complicated manner, in that it initially breaks into three filaments, which fuse into two asymmetric beams, to give the final two filaments. However, depending on the values of initial parameters, the size of the vortex and its charge, the break-up of both isotropic models, as well as the anisotropic model, can result in more than two fragments.

Finally, it is worthwhile mentioning that the angular momentum of the vortex in the anisotropic model is not conserved. It drops fast as the vortex disintegrates, and oscillates about zero. The angular momentum of the vortices in isotropic models is conserved as long as the vortices are intact, however it starts slowly to decrease during and after the break-up phase, owing to the radiation that takes away part of the angular momentum and of the power of the system (Fig. 4).

7. Conclusions

In conclusion, we have obtained a new analytical expression for the 2D space-charge field in PR crystals, appropriate to the propagation of self-trapped optical beams. Based on this expression, an improved model for the local isotropic space-charge field in 2D is proposed, that agrees better with the numerical solution. We test the model, together with the standard inverse-intensity local model, on the problem of the break-up of vortex beams in PR crystals, which is known to exhibit very different behavior in the local and nonlocal models. It is found that the vortices in isotropic models exhibit a much more stable propagation than the vortices in the anisotropic model, eventually breaking into two or more filaments that fly apart. The vortex of charge 1 in the anisotropic model breaks right away into two filaments that fly apart along the stable direction perpendicular to the external field.

In isotropic models the power and the angular momentum of stable self-trapped beams are conserved. In numerical simulations the power and the angular momentum of propagating beams may become not conserved, if the beams suffer instability. In the case of vortices, they remain constant as long as the shape of the vortex is preserved, but when the vortex starts disintegrating, it radiates more strongly, and the part of power and angular momentum is lost to radiation. Since we are using absorbing boundary conditions at the transverse edges of the computational domain, the values of power and angular momentum start decreasing after the break-up of vortex. Similar findings have been reported for the case of spiraling solitary waves [12,14]. On the other hand, the angular momentum of the anisotropic model is not conserved from the beginning, since the model represents a noncentral mechanical system in the transverse plane. For such a nonintegrable model, there is no reason for the angular momentum to be conserved.

Acknowledgements

Support from the Spanish Comisión Interministerial de Ciencia y Tecnología, and from the Comunidad de Madrid is gratefully acknowledged. G.F.C. acknowledges an F.P.I. grant from the Ministerio de Ciencia y Tecnología, and M.R.B. is thankful to IBERDROLA for the visiting professorship at the Universidad Autónoma de Madrid. Work at the Institute of Physics is supported by the Ministry of Science, Technologies, and Development of the Republic of Serbia, under the project OI 1475.

References

[1] A short review is provided by G.I. Stegeman, M. Segev, Science 286 (1999) 1518, For an overview, see the Special Issue on solitons, Ed. M. Segev, Opt. Phot. News 13 (2) (2002).
[2] A.A. Zozulya, D.Z. Anderson, Phys. Rev. A 51 (1995) 1520.
[3] B. Crosignani, P. Di Porto, A. Degasperis, M. Segev, S. Trillo, J. Opt. Soc. Am. B 14 (1997) 3078.
[4] A. Stepken, F. Kaiser, M. Belić, J. Opt. Soc. Am. B 17 (2000) 68.
[5] L. Solymar, D.J. Webb, A. Grunnet-Jepsen, The Physics and Applications of Photorefractive Materials, Claredon Press, Oxford, 1996.
[6] G.F. Calvo, B.I. Sturman, F. Agulló-López, M. Carrascosa, Phys. Rev. Lett. 84 (2000) 3839.
[7] D.N. Christodoulides, S.R. Singh, M.I. Carvalho, M. Segev, Appl. Phys. Lett. 68 (1996) 1763.
[8] A.V. Buryak, Yu.S. Kivshar, M. Shih, M. Segev, Phys. Rev. Lett. 82 (1999) 81.
[9] J.J. Garcia-Ripoll, V.M. Perez-Garcia, E.A. Ostrovskaya, Yu.S. Kivshar, Phys. Rev. Lett. 85 (2000) 82.
[10] W. Krolikowski, E.A. Ostrovskaya, C. Weilnau, M. Geisser, G. McCarthy, Yu.S. Kivshar, C. Denz, B. Luther-Davies, Phys. Rev. Lett. 85 (2000) 1424.
[11] T. Carmon, R. Uzdin, C. Pigier, Z.M. Musslimani, M. Segev, A. Nepomnyashchy, Phys. Rev. Lett. 87 (2001) 143910.
[12] M.R. Belić, D. Vujić, A. Stepken, F. Kaiser, G.F. Calvo, F. Agullo-Lopez, M. Carrascosa, Phys. Rev. E 65 (2002) 066610.
[13] C. Weilnau, M. Ahles, J. Petter, D. Träger, J. Schröder, C. Denz, Ann. Phys. (Leipzig) 11 (2002) 573.
[14] D.V. Skryabin, J.M. McSloy, W.J. Firth, Phys. Rev. E 66 (2002) 055602(R).